Journal of Porous Materials 12: 337–343, 2005


# Preparation of Polyaniline/Mesoporous Silica Hybrid and Its Electrochemical Properties

TAKAHIRO TAKEI*, KOHEI YOSHIMURA, YOSHINORI YONESAKI, NOBUHIRO KUMADA AND NOBUKAZU KINOMURA

*Center for Crystal Science and Technology, Faculty of Engineering, University of Yamanashi, 7 Miyamae, Kofu, Yamanashi 400-8511, Japan*

takei@yamanashi.ac.jp

*Received October 27, 2004; Revised April 6, 2005*

**Abstract.** Polyaniline/mesoporous silica hybrids were prepared by chemical modification with aniline and their capacitances were examined for application to electrode of electrochemical capacitor. The chemical modification was performed by two kinds of processes, polymer insertion into pores and in-situ polymerization within pores. In the case of the polymer insertion process, since the mean pore sizes of the hybrid did not change, polyaniline molecules were not inserted. On the other hand, in the case of the in-situ polymerization process, the mean pore sizes decreased from that of mesoporous silica, while the XRD patterns became broad. Therefore, aniline molecules polymerized in the inside of pores, however, the mesoporous silica collapsed in part. Maximum capacitance measured in 1 mol/l $H_2SO_4$ aqueous solution was around 226 F per unit mass of polyaniline.

**Keywords:** polyaniline, mesoporous silica, hybrid, electrochemical property, capacitance

## 1. Introduction

An electrochemical capacitor is a remarkable device because it has potentially larger capacitance than conventional capacitors. Generally, capacitors have the advantage of high specific power and a faster rate of electric charging and discharging than secondary batteries. However, electrolytic capacitors have low specific energy, while Ni-MH or Li ion batteries have high specific energy. Therefore, further increases in specific energy would be desirable for the capacitor to serve as a replacement for secondary batteries.

In the case of electrochemical capacitors, both electric double layer [1, 2] and redox capacitance [3, 4] have been investigated by many researchers. For electric double layer capacitors, charging is carried out by forming the electric double layer at the surface of the electrode. In this case, high specific surface area is necessary for large capacitance because high surface area makes the electric double layer extensive. Generally, activated carbon has been investigated for such an electrode [5, 6] due to its high surface area and electric conductivity. On the other hand, in the case of the redox capacitor, charging is carried out by redox reactions between the surface and the solution. In this case, these redox reactions in the range of limited voltage are necessary for capacitor-like behavior. The charging occurs predominantly by the redox reaction and diffusion of electrolyte to the electrode. Therefore, high specific surface area and quick redox reactions are necessary for efficient charging of the redox capacitor. For the redox capacitor, $RuO_2$ [7, 8], NiO [3], other transition metal oxides [9] or some kinds of conductive polymers [10, 11] have been studied.

In producing electrodes of redox capacitors of conductive polymers, a film form has been generally used in order to enlarge its surface area. However, in this film format it has generally been difficult to achieve

*To whom correspondence should be addressed.

a sufficiently high surface area for the huge capacitance demanded. On the other hand, hybridization of the conductive polymer which can be used with mesoporous supporting materials with high surface area may be an interesting means for enlarging capacitance. In this paper, preparation of polyaniline/mesoporous silica hybrid was examined and its electrochemical properties investigated.

## 2. Experimental

### *2.1. Preparation of Mesoporous Silica*

Mesoporous silica (MPS) as a starting material was prepared by the following process. Cetyltrimethylammonium bromide (CTAB) was dissolved completely with distilled water. Tetraethoxysilane (TEOS) was dropped into the solution with stirring. Ethylamine was used as a basic catalyst for hydrolysis and polymerization of TEOS. The components, TEOS, CTAB, ethylamine and $H_2O$ were used with a composition of 7.6 : 1.0 : 13.1 : 944.0 molar ratio. After stirring for 10 min., the mixed solution was hydrothermally treated at 110°C for 48 h in a Teflon-sealed vessel. The resultant aggregates dried at 50°C were placed into an ethanol solution containing 20 vol% of 5 mol/l HCl for removal of CTAB. Consequently, the treated product was used as MPS.

### *2.2. Preparation of Hybrid*

The hybridization processes was carried out via two methods designated as PI and EP.

In the PI process, polyaniline (PAn) was synthesized precedently by the process as follows. Aniline, 5 mol/l HCl and ethanol were mixed with the volume ratio of 2 : 5 : 20 and kept at 0°C. The catalytic reagent for polymerization used in this study was a 1 mol/l ammonium peroxodisulfate ($(NH_4)_2S_2O_8$) aqueous solution under acidic condition. These solutions were blended and stirred at 0°C for 2 h. The product was washed with distilled water and dried at 50°C and the resultant product was used as PAn. The synthesized PAn was placed into $NH_4OH$ solution to reduce PAn. Its color changed from green to blue and its conductivity was lost. The reduced PAn was able to be dissolved in 1-methyl-2-pyrrolidone ($CH_3NC_4H_6O$). The MPS was added to the PAn solution at an aniline/silica ratio of 1.0–6.0. The mixed solution was shaken at 40°C for 48 h at 200 rpm for inserting PAn into the pores. After the insertion process, the sample was washed with 1-methyl-2-pyrrolidone and ethanol, and dried at 50°C.

*Table 1.* Loaded ratio of PAn per MPS.

| Sample name | PI1 | PI2 | PI3 | EP1 | EP2 | EP3 |
|---|---|---|---|---|---|---|
| Loaded PAn per MPS | 1.0 | 3.0 | 6.0 | 3.3 | 6.6 | 13.3 |

The EP process was carried out as follows. MPS was placed into unpolymerized aniline aqueous solution with an aniline/silica molar ratio of 3.3–13.3 under acidic conditions and stirred for 2 h in order to disperse and impregnate aniline with MPS. After the impregnation treatment, the ammonium peroxodisulfate aqueous solution was blended and stirred at 0°C for 2 h for polymerization. The resulting polymerized aniline/MPS hybrid particles have not only PAn inserted in the pores but also excess PAn on the external surface of MPS particles. Therefore, the hybrids were put into 1-methyl-2-pyrrolidone and were shaken at 40°C for 2 h for removing excess PAn.

The loaded ratios of aniline to MPS examined here were listed in Table 1.

### *2.3. Characterization*

The structure of the hybrids was examined by powder XRD (MXP$^3$, MacScience) with CuK$\alpha$ radiation monochromated by Ni filter. The specific surface area, pore volume and pore size distribution were evaluated by microporosimeter (BELSORP28SA and BELSORP mini, BEL japan) using $N_2$ adsorption at 77 K. The state of PAn was investigated by FT-IR spectroscopy (FT/IR-410, Jasco) using a KBr pellet method and UV-vis spectroscopy (V-550, Jasco). The amount of PAn contained in the sample was examined by TG-DTA (TG8101D, Rigaku).

The electrochemical properties were examined by a potentiostat and a function generator (HA-301 and HB-104, Hokuto denko) with a SCE reference electrode in 1 mol/l $H_2SO_4$ aqueous solution. The measurement of cyclic voltammograms was performed with sweep range of voltage from −0.25 to 1.00 V at the rate of 1 or 20 mV/sec.

For preparation of electrode, a sample powder (200 mg) was compacted to 1.0 cm in diameter using a uniaxial press at 255 MPa.

## 3. Results

Figure 1 shows the XRD pattern and pore size distribution of MPS prepared as the starting material.

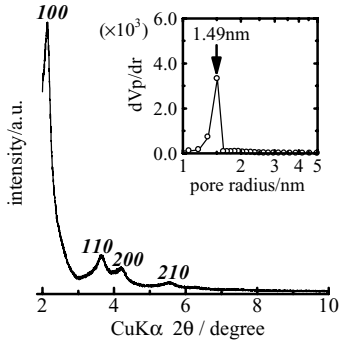


*Figure 1.* XRD pattern and pore size distribution of MPS.

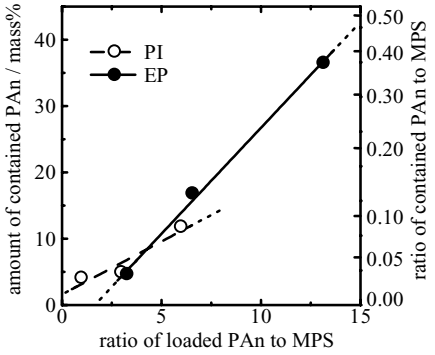


*Figure 3.* Relationship between loaded PAn to $SiO_2$ and contained amount of PAn in the hybrids.

From the diffraction pattern, the diffraction lines of 100, 110 and 200 were apparently confirmed. Therefore, the prepared MPS was found to have a hexagonal structure with lattice constant of 4.8 nm. Specific surface area of around 920 $m^2/g$ and mean pore radius of around 1.5 nm were evaluated from adsorption isotherm by BET and DH method, respectively.

UV-vis spectra of the hybrids are shown in Fig. 2. Two kinds of characteristic absorption at around 250–400 and around 480–750 were observed in these spectra. These two adsorption bands could be assigned as follows; $\pi$-$\pi$* transition of the benzenoid ring at around 320 nm and exciton adsorption of quinoid ring at around 630 nm [13].

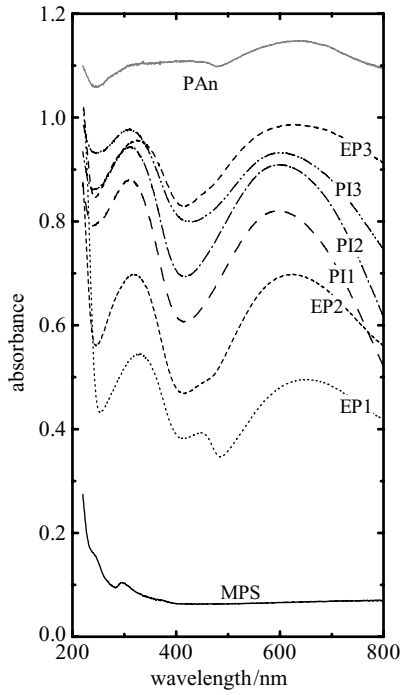


*Figure 2.* UV-vis spectra of PAn/MPS prepared by PI and EP method with various compositions.

Figure 3 shows the relationships between loaded ratio of PAn to MPS and amount of PAn contained in the hybrids. The plots for PI and EP are indicated by dashed and solid lines, respectively. From these plots, the amount of included PAn was found to increase with loading ratio for both samples. However, slopes of these lines were different between PI and EP samples. The hybridization of EP samples seems to occur more efficiently than that of PI. Since PI3 and EP3 samples had the maximum amount of PAn in the hybrids from each preparation method, these samples were used for investigating their porous properties and capacitance.

Figure 4shows the XRD patterns of the MPS, PI3 and EP3 hybrids. The PI3 hybrids seems to keep its hexagonal structure completely, while the EP3 sample becomes a little disordered which can be seen from

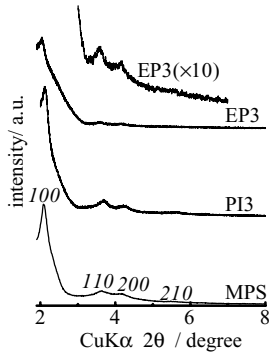


*Figure 4.* XRD patterns MPS, PAn, PI3 and EP3.

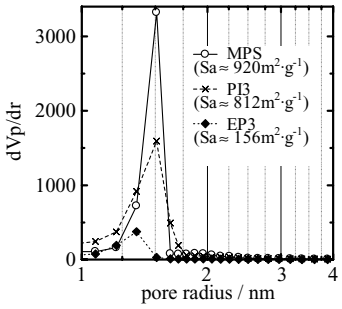


*Figure 5*. Pore size distributions of MPS, PAn, PI3 and EP3.

the broadening and decrease in intensity of diffraction peaks. However, lattice constants of these samples were very similar. Figure 5shows pore size distributions of MPS, PI3 and EP3 hybrids with specific surface area. Comparisons between MPS and PI3, since main pore size of 1.51 nm were similar, it would appear that PAn could not be inserted into pores of the PI3 sample. On the other hand, the main pore size of EP3 is smaller than that of MPS. Therefore, the aniline monomer could be inserted into the pores and in-situ polymerized. Specific surface area of EP3 is much lower than that of the MPS. This decrease indicates a partial collapse of the hexagonal structure corresponding to the XRD patterns in Fig. 4.

Electrochemical properties were examined via cyclic voltammograms. Figures 6(a)and (b) show the cyclic voltammograms of MPS, PAn, PI3 and EP3 samples at a sweep rate of 20 mV/sec and those of PAn and EP3 at a rate of 1 mV/sec, respectively. In Fig. 6(a), measured voltammograms did not seem to be rectangle, and redox peaks corresponding to the oxidation/reduction of PAn were not apparent. On the contrary, in Fig. 6(b) taken with slower sweep rates, some redox peaks of PAn appear. The cause of the appearance of the redox peaks will be discussed later. The capacitance per unit mass of hybrid, $C$, and that per unit mass of aniline, $C_A$, of the PI3 and EP3 hybrids were evaluated from these voltammograms using equation reported by Zheng et al. [7] as shown in Table 2.

*Table 2*. Measured capacitances of MPS, PAn, PI3 and EP3.

| Sample | MPS | PAn | PI3 | EP3 | PAn | EP3 |
|---|---|---|---|---|---|---|
| sweep rate/ mV·sec$^{-1}$ | | 20 | | | 1 | |
| $C$/F·g$^{-1}$ | 0.2 | 3.7 | 0.6 | 8.1 | 27.9 | 82.4 |
| $C_A$/F·g$^{-1}$ | — | 3.7 | 5.1 | 22.3 | 27.9 | 225.8 |

## 4. Discussion

### *4.1. State of Polyaniline*

As shown in Fig. 2, $\pi$-$\pi$* transition of the benzenoid rings observed at around 320 nm and exciton adsorption of quinoid rings observed at around 630 nm. The absorbance at 320 and 630 nm are designated as $A_{320}$ and $A_{630}$, respectively. In the spectra of PAn, $A_{630}$ is apparently larger than $A_{320}$. $A_{320}$ was always larger than $A_{630}$ in the case of PI samples, while in the case of EP samples $A_{630}$ increased more steeply than $A_{320}$ with amount of PAn and $A_{630}$ finally became larger than $A_{320}$. The constant $A_{630}/A_{320}$ ratio of PI samples suggests that a fraction of the quinoid rings in a molecule of PAn did not change with the loaded amount of PAn in the PI treatment. On the other hand, in the case of EP

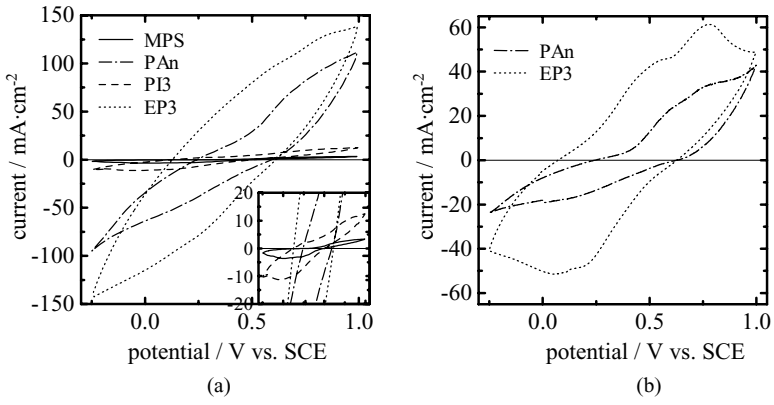


*Figure 6*. Cyclic voltammograms of MPS, PAn, PI3 and EP3. (a) sweep rate: 20 mV/sec (b) sweep rate: 1 mV/sec.

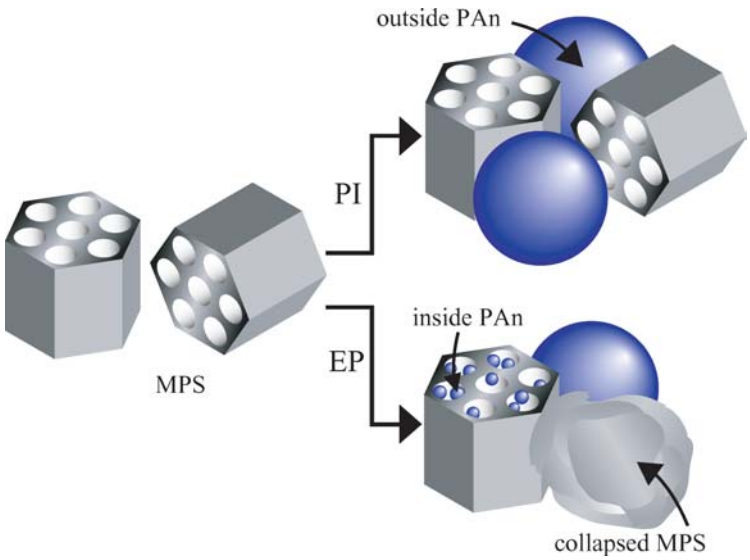


*Figure 7.* Schematic illustration of the hybridization via PI and EP method.

samples, the amount of quinoid rings have the tendency to increase depending on the amount of loaded aniline, that is, MPS affects molecular state of polymerized PAn.

### 4.2. *Texture of Hybrids*

Textures of hybrids are investigated from their $S_a$s, pore size distributions and the amount of PAn in the hybrids. As mentioned above, mean pore size did not change in the PI treatment, while decreased in the EP treatment. In order to investigate their hybridized structure in detail, mass amount of the MPS, collapsed MPS, PAn in the inside of pore and on the outer surface are calculated from the specific surface area, pore volume, mean pore size and amount of PAn evaluated via TG curve using following simultaneous equations;

$$V_P = V_{P(\mathrm{MPS})} \cdot M_{\mathrm{MPS}} - \frac{M_{\mathrm{PAn}}}{D_{(\mathrm{PAn})}} = V_{P(\mathrm{MPS})} \cdot M_{\mathrm{MPS}} \cdot \left(\frac{R_P}{R_{P(\mathrm{MPS})}}\right)^2$$

where $M_{\mathrm{MPS}}$ and $M_{\mathrm{PAn}}$ are the mass fraction of the included MPS and the PAn in the inside of pore of the hybrid, $D_{(\mathrm{PAn})}$ is density of PAn of 1.244 g/cm$^3$ referred from Stejskal et al. [13], $V_{p(\mathrm{MPS})}$ and $V_p$ are pore volume, $R_{p(\mathrm{MPS})}$ and $R_p$ are mean pore radius of the MPS and the hybrid. This calculation was performed assuming; particles of collapsed MPS and outside PAn are dense and large so their specific surface areas are ignorable, and collapsed MPS is not including the outside PAn. Table 3shows the calculated mass fractions. From the Table 3, both amount of the PAn in the inside of pores and that of the collapsed MPS are very small for PI3. Therefore, the PI treatment resulted in the formation of a mixture of MPS and PAn particles. On the other hand, it is found that the ratio of the PAn in the inside of the pores on total PAn is around 0.1 and the ratio of the collapsed MPS on total silica is around 0.7 for EP3 hybrid. That is, a part of PAn is surely inserted into pores of the MPS and a large fraction of MPS collapsed. The schematic illustration of these texture models are shown in Fig. 7.

*Table 3.* Mass fractions of included MPS, collapsed MPS, inside and outside PAn in pores of the hybrids.

| Sample name | MPS | PI3 | EP3 |
|---|---|---|---|
| $S_a$/m$^2$·g$^{-1}$ | 920 | 812 | 156 |
| $V_p$/ml·g$^{-1}$ | 0.763 | 0.666 | 0.115 |
| $R_p$/nm | 1.51 | 1.51 | 1.35 |
| MPS | | | |
| included ($M_{\mathrm{MPS}}$)/mass% | 100.0 | 86.6 | 18.9 |
| collapsed/mass% | 0.0 | 1.6 | 44.6 |
| PAn | | | |
| inside ($M_{\mathrm{PAn}}$)/mass% | 0.0 | 0.0 | 3.6 |
| outside/mass% | 0.0 | 11.8 | 32.9 |

### *4.3. Electrochemical Property*

The cyclicvoltammograms of the PAn, PI3 and EP3 samples at the constant sweep rate of 20 mV/sec are shown in Fig. 6(a). The current at 1.0 V in the voltammogram of the PI3 was around one ninth and one eleventh of that of the PAn and EP3 samples. In this paper, it was assumed that particles of the outside PAn were large and their specific surface area was ignorable as mentioned before. Since the mass fraction of the outside PAn in the PI3 is around 12 mass%, the current of the PI3 corresponds to the mass fraction of the outside PAn in comparison with that of the PAn sample. As shown in Table 2, the $C$ of the PI3 was also smaller than that of the PAn sample because the inside PAn was inexistent in the PI3. On the other hand, the $C$ of the EP3 sample was more than twice as large as that of the PAn. It was surprisingly large in value contrary to the small amount of the inside PAn of around 4 mass%. That is, no more than a small amount of the inside PAn contributes acceleration of $C$ due to its high dispersion in the pores of MPS.

In order to consider dependence of cyclicvoltammograms on their sweep rate, the voltammograms at different sweep rate as shown in Figs. 6(a) and (b) were compared in detail. Ratio of these sweep rates of 20 to 1 mV/sec are twenty, so the current in the voltammogram at 1 mV/sec ought to be similar to the current divided by twenty at 20 mV/sec. However, the current at 1 mV/sec was extraordinarily large and was around half of that at 20 mV/sec. The voltammogram at 1 mV/sec has more distinct redox peaks which appeared at around 0.53 and 0.77 V on a positive and 0.20 and 0.06 V on a negative sweep than that at 20 mV/sec. Parts of two of the four peaks at lower voltage, 0.53 and 0.06 V, are derived from redox reaction of doping anion to form polaron. The other two peaks at higher voltage, 0.77 and 0.20 V, are attributed to change of conductive carrier from polaron to bipolaron.[10, 11, 14–17]

Since the ratio of the current of the voltammograms at 1 to that at 20 mV/sec was much larger than that of the sweep rates of 1 to 20 mV/sec, the $C$ became very large at a slow sweep rate. In this paper, as sulfuric acid aqueous solution was used, the dopant was $SO_4^{2-}$ anion of which the diffusion reaction was considered to be predominant for charging and discharging. Therefore, this dependence of the $C$ on the sweep rate could be considered to be derived from the predominance of diffusion of $SO_4^{2-}$ for the hybrids. That is, the redox multi-reaction is necessary to occur for capacitor-like behavior, however the redox reactions had not saturated at fast sweep rate of 20 mV/sec due to the slow diffusion.

In order to investigate the effect of dispersion of the PAn clearly, the capacitances per mass of PAn, $C_A$ were compared between the PAn and the EP3 of around 28 and 226 F/g calculated from the voltammograms at 1 mV/sec, respectively. The $C_A$ of the PAn was around eight times as small as that of the EP3. Considering that the fraction of inside PAn of the pores was around 0.1 on existing PAn, the $C_A$ of the EP3 seems to be very large. Therefore, increase of inside PAn of the pores without collapse of the porous texture and shortening the diffusion path for dopant anion should be investigated in the future study.

## 5. Conclusions

PAn/MPS hybrid was prepared and its electrochemical properties were examined with the following results.

1. PAn/MPS could be prepared by in-situ polymerization with maximum amount of PAn of around 37 mass%.
2. Diffusion of $SO_4^{2-}$ ion is considered to dominate the electrochemical properties of the hybrids.
3. High dispersion of PAn with nano size accelerated the electrochemical capacity.
4. The maximum capacitance per 1 g of PAn contained in the hybrid was around 226 F.

## Acknowledgment

This research was partially supported by the Nippon Sheet Glass Foundation for Materials Science and Engineering.

## References

1. D. Qu, J. Power Sources **109**, 403 (2002).
2. M. Arulepp, L. Permann, J. Leis, A. Perkson, K. Rumma, A. Jänes, and E. Lust, J. Power Sources **133**, 320 (2004).
3. K.-C. Liu and M.A. Anderson, J. Electrocherm. Soc. **143**, 124 (1996).
4. W.-C. Chen, C.-C. Hu, C.-C. Wang, and C.-K. Min, J. Power Sources **125**, 292 (2004).
5. A. K. Chatterjee, M. Sharon, R. Banerjee, and M. Eumann-Spallart, Electrochimica Acta **48**, 3439 (2003).
6. S. Mitani, S.-I. Lee, S.-H. Yoon, Y. Korai, and I. Mochida, J. Power Sources **133**, 298 (2004).

7. J.P. Zheng, P.J. Cygan, and T.R. Jow, J. Electrocherm. Soc. **142**, 2699 (1995).
8. Y. Takasu and Y. Murakami, Electrochimica Acta **45**, 4145 (2000).
9. L. Kavan, M. Grätzel, J. Rathouský, and A. Zukal, J. Electrocherm. Soc. **143**, 394 (1996).
10. C.-C. Hu and C.-H. Chu, Mater. Chem. Phys. **65**, 329 (2000).
11. C.-C. Hu, E. Chen, and J. Y. Lin, Electrochimica Acta **47**, 2741 (2002).
12. F. Yan and G. Xue, J. Mater. Chem. **9**, 3035 (1999).
13. J. Stejskal and R.G. Gilbert, Pure Appl. Chem. **74**, 857 (2002).
14. Y.-B. Shim, M.-S. Won, and S.-M. Park, J. Electrocherm. Soc. **137**, 538 (1990).
15. D.E. Stilwell and S.-M. Park, J. Electrocherm. Soc. **135**, 2497 (1988).
16. T. Kobayashi, H. Yoneyama, and H. Tamura, J. Electroanal. Chem. **177**, 291 (1984).
17. Z. Jiang, X. Zhang, and Y. Xiang, J. Electroanal. Chem. **351**, 321 (1993).